A "triple sea-ice state" mechanism for the abrupt warming and synchronous ice sheet collapses during Heinrich events

Yohai Kaspi

Department of Earth Atmospheric and Planetary Sciences, Massachusetts Institute of Technology, Cambridge, Massachusetts, USA

Roiy Sayag and Eli Tziperman

Department of Earth and Planetary Sciences and Division of Engineering and Applied Sciences, Harvard University, Cambridge, Massachusetts, USA

Received 21 January 2004; revised 10 May 2004; accepted 25 May 2004; published 14 July 2004.

[1] Abrupt, switch-like, changes in sea ice cover are proposed as a mechanism for the large-amplitude abrupt warming that seemed to have occurred after each Heinrich event. Sea ice changes are also used to explain the colder-than-ambient glacial conditions around the time of the glacier discharge. The abrupt warming events occur in this mechanism, owing to rapid sea ice melting which warmed the atmosphere via the strong sea ice albedo and insulating feedbacks. Such abrupt sea ice changes can also account for the warming observed during Dansgaard-Oeschger events. The sea ice changes are caused by a weak (order of 5 Sv) response of the thermohaline circulation (THC) to glacier discharges. The main point of this work is therefore that sea ice may be thought of as a very effective amplifier of a weak THC variability, explaining the abrupt temperature changes over Greenland. Synchronous ice sheet collapses from different ice sheets around the North Atlantic, indicated by some proxy records, are shown to be possible via the weak coupling between the different ice sheets by the atmospheric temperature changes caused by the sea ice changes. This weak coupling can lead to a "nonlinear phase locking" of the different ice sheets which therefore discharge synchronously. It is shown that the phase locking may also lead to "precursor" glacier discharge events from smaller ice sheets before the Laurentide Ice Sheet discharges. The precursor events in this mechanism are the result rather than the cause of the major glacier discharges from the Laurentide Ice Sheet. *INDEX TERMS:* 1620 Global Change: Climate dynamics (3309); 1635 Global Change: Oceans (4203); 1863 Hydrology: Snow and ice (1827); 3339 Meteorology and Atmospheric Dynamics: Ocean/atmosphere interactions (0312, 4504); 3344 Meteorology and Atmospheric Dynamics: Paleoclimatology; *KEYWORDS:* sea ice, Heinrich events, Dansgaard-Oeschger events

Citation: Kaspi, Y., R. Sayag, and E. Tziperman (2004), A "triple sea-ice state" mechanism for the abrupt warming and synchronous ice sheet collapses during Heinrich events, *Paleoceanography*, *19*, PA3004, doi:10.1029/2004PA001009.

1. Introduction

[2] The dramatic Heinrich events, involving major glacier discharges from the Laurentide Ice Sheet (LIS) every 7000–10000 years, have dominated climate variability during the last glacial period. The glacier discharges that have occurred during Heinrich events [*Heinrich*, 1988; *Broecker et al.*, 1992; *Bond et al.*, 1992] have been explained by *MacAyeal* [1993b] using a "binge-purge" mechanism. In the proposed scenario, as the Laurentide Ice Sheet (LIS) thickened in the region of Hudson Bay due to snow accumulation (binge, or growth, stage), geothermal heat was trapped at the base of the ice sheet due to the thick and insulating glacier that prevented it from escaping to the atmosphere. Eventually, the geothermal heating led to basal melting, which reduced the friction of the ice sheet with its bottom boundary and caused the glacier discharge into the Labrador Sea and the North Atlantic ocean (purge, or collapse, stage). The thinner glacier then allowed the geothermal heat to diffuse out, so that the base could refreeze, and the cycle repeated.

[3] There have been several attempts to explain the Heinrich and Dansgaard Oeschger (D/O) events using externally specified stochastic or periodic freshwater pulses through their effects on the thermohaline circulation (THC) [*Paillard and Labeyrie*, 1994; *Alley et al.*, 2001; *Ganopolski and Rahmstorf*, 2001; *Timmermann et al.*, 2003]. However, having to specify the freshwater forcing rather than explaining it as part of the mechanism clearly leaves more to be desired. In addition, some of the proposed mechanisms [*Ganopolski and Rahmstorf*, 2001] require very large-amplitude THC changes (up to nearly 50 Sv).

[4] The proxy record shows evidence for synchronous discharges of several different ice sheets around the Atlantic, including from the Hudson Bay (LIS), the Icelandic Ice Sheet, Gulf of St. Lawrence, the British Ice Sheet, the Barents Sea Ice Sheet, and possibly also the Fennoscandian Ice Sheet [*Bond and Lotti*, 1995; *Elliot et al.*, 1998; *Fronval et al.*, 1995; *McCabe and Clark*, 1998; *Bischof*, 1994; *Jones and Keigwin*, 1988]. The synchronized discharge from the

0883-8305/04/2004PA001009$12.00

different ice sheets is especially surprising in view of MacAyeal's mechanism, as this mechanism is based on an insulation of the glacier's base from its environment and therefore seemingly forbids any communication between different ice sheets that may lead to a synchronization between them.

[5] There is also some evidence for "precursor" events, in which a small ice sheet discharges glaciers just before a major discharge from the LIS, as seen, e.g., for the Iceland Ice Sheet [*Bond and Lotti*, 1995; *Bond et al.*, 1999; *Scourse et al.*, 2000; *Grousset et al.*, 2000]. If these precursor events are indeed linked to the major discharges from the LIS, this rules out a link between the ice sheets via sea level changes. It seems unlikely that a small discharge from a small ice sheet will be sufficient to trigger a large LIS discharge.

[6] We present here a mechanism that accounts for the abrupt warming events [*Dansgaard et al.*, 1993; *Bond et al.*, 1993] which seem to start a few hundred years after each ice-rafted debris (IRD) discharge and last for about 1000 years. The proposed mechanism also accounts for the cold periods that seem to accompany the glacier discharge events [*Bard et al.*, 2000; *Bond et al.*, 1993; *Broecker and Hemming*, 2001]. We show this mechanism using two independent models. First, a box model that, although simple, fully couples the dynamics of the ice sheets, atmosphere, ocean ice, and sea ice, all of which participate in the proposed mechanism (the model is much simpler than, e.g., the coupled "Earth system" models of *Weaver et al.* [2001] and *Wang and Mysak* [2001]. Second, a more detailed coupled ocean-atmosphere-sea ice-land ice model which is continuous in the meridional dimension. On the basis of the proposed mechanism, we then also explain the synchronized collapses by coupling together different ice sheets via the other climate system components.

[7] It should be mentioned that there are quite a few recent papers which suggest no synchronous collapses of glaciers into the North Atlantic [e.g., *Dowdeswell et al.*, 1999; *Sarnthein et al.*, 2000]. The binge/purge mechanism seems to contradict synchronous collapses, as it requires the ice sheet bases to be insulated from their environments. Our objective in presenting a mechanism for synchronous events is to show that such synchronous behavior is dynamically possible in principle. Should synchronous collapses be ruled out eventually, this should therefore occur, owing to more concrete future observations rather than due to dynamical reasons. As for the binge/purge oscillator itself, there are several criticisms to that being a realistic mechanism for the Heinrich events [*Marshall and Clarke*, 1997; *Clarke et al.*, 1999]. Some alternative theories are reviewed in the work of *Alley and Clark* [1999] and *Maslin et al.* [2001]. We emphasize that the main messages of this paper: that sea ice is the cause of abrupt temperature changes observed as part of the D/O and Heinrich events in the Greenland ice cores, and is an efficient amplifier of THC variability, is independent of the synchronous collapses issue, and should be a robust finding of this study.

[8] A brief model description follows in section 2, and full details are given in Appendix A. Then the proposed Heinrich cycle mechanism is explained in section 3, the synchronous discharges are discussed in section 4, and the role of the THC is examined in section 5. We conclude in section 6.

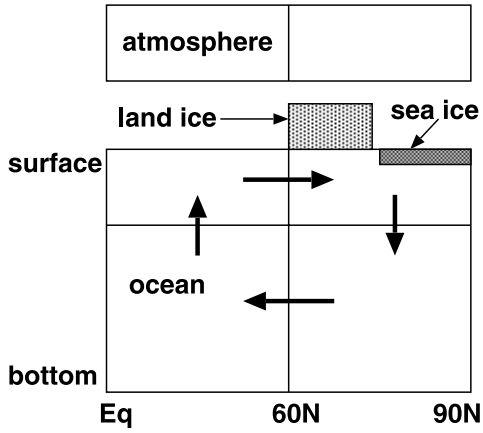

Figure 1. A schematic diagram of the coupled box model, showing the ocean, atmosphere, sea ice, and land ice components. Several land ice sheets are in fact implemented and used in the runs described in the text. The arrows mark the direction of the THC.

2. The Models

[9] The coupled box model is schematically shown in Figure 1. *MacAyeal*'s [1993b] binge/purge oscillator is used to represent the land ice component in our model. Since we use a fully coupled model, the snow accumulation rate and the atmospheric temperature as function of time are not specified as in the work of *MacAyeal* [1993b] but are determined by the atmospheric model. Similarly, the land ice model determines the rate and volume of the freshwater flux into the ocean model during the purge stage. Using MacAyeal's land ice model rather than an ice sheet model as used for example by *Gildor and Tziperman* [2001] implies, of course, that we can only address millennial, rather than glacial-interglacial, timescales. While there is a debate regarding the details of this model and its implied freshwater pulse into the ocean [*Marshall and Clarke*, 1997; *Clarke et al.*, 1999], we note that an alternative model with a different mechanism for the periodic collapses of the LIS may easily be incorporated in our coupled model. Furthermore, we find that a significantly weaker freshwater pulse does not qualitatively affect our proposed mechanism for abrupt atmospheric warming events and synchronous discharges.

[10] The ocean is represented in our simpler coupled model by a standard Northern Hemispheric meridional four-box model [*Stommel*, 1961; *Huang et al.*, 1992], including a sea ice component as in the work of *Gildor and Tziperman* [2000]. The thermohaline circulation is calculated in the standard fashion from the meridional density gradient and is constrained to be above 6 Sv (this limit is shown below not to affect our results and is not used nor needed in the continuous coupled model used here). The temperature and salinity for each box are calculated using

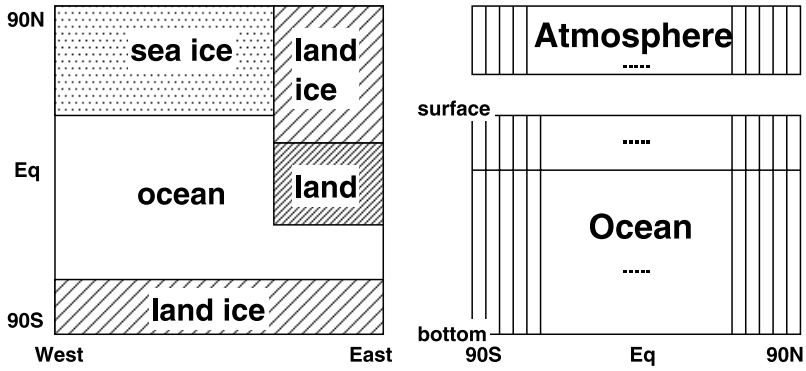

Figure 2. Top and side views of the coupled, pole-to-pole, zonally averaged, and ocean-atmosphere-sea ice-land ice model with continuous meridional resolution.

advection diffusion equations that are forced at the surface by air-sea heat fluxes, and by freshwater fluxes from atmospheric precipitation, glacier runoff (during the ice sheet collapse stage), and sea ice formation and melting. Convective mixing is used to vertically mix the boxes once the vertical stratification becomes unstable. Sea ice plays a major dynamical role here through its strong albedo effect, which dominates the atmospheric energy balance, and by insulating the ocean from the atmosphere and significantly reducing the air-sea fluxes where sea ice cover is present. The atmospheric model is a simple two-box energy balance model [*Nakamura et al.*, 1994; *Gildor and Tziperman*, 2000]. The temperature at a given box is determined by the balance between the incoming shortwave radiation, outgoing longwave radiation, air-sea fluxes, and meridional atmospheric heat fluxes.

[11] The second model used here, is a coupled ocean-atmosphere-sea ice model that is continuous in the latitudinal direction yet similar otherwise to the simpler box model described above. The model was developed and used by *Sayag* [2003] and *Sayag et al.* [2004], is schematically shown in Figure 2, and is used below to verify the robustness of the proposed mechanism to the model resolution. Unlike the simpler box model, this model was not used with an active land ice component and therefore does not produce Heinrich events spontaneously like the simpler model. In the experiments described below, this model is therefore forced by freshwater pulses emulating the glacier discharges to produce the sea ice response in which we are interested here and to strengthen the results of the simpler model. A more detailed description of both models is given in Appendix A.

3. The Proposed Heinrich Cycle Mechanism

[12] Figure 3 shows the different components of the climate system during a complete model Heinrich cycle in our fully coupled (ice sheet, ocean, atmosphere, and sea ice) simple box model. Figure 4 shows a full cycle of the ocean, atmosphere, and sea ice components in our detailed meridionally continuous model, driven by specified periodic freshwater pulses every 6000 years, which simulate the glacier discharges calculated explicitly in the simpler model. The ice sheet oscillations in our model are essentially like those of *MacAyeal* [1993b]. Figure 3a shows how the accumulation (growth) stage ends when the base temperature, constantly heated by the geothermal heat flux, has

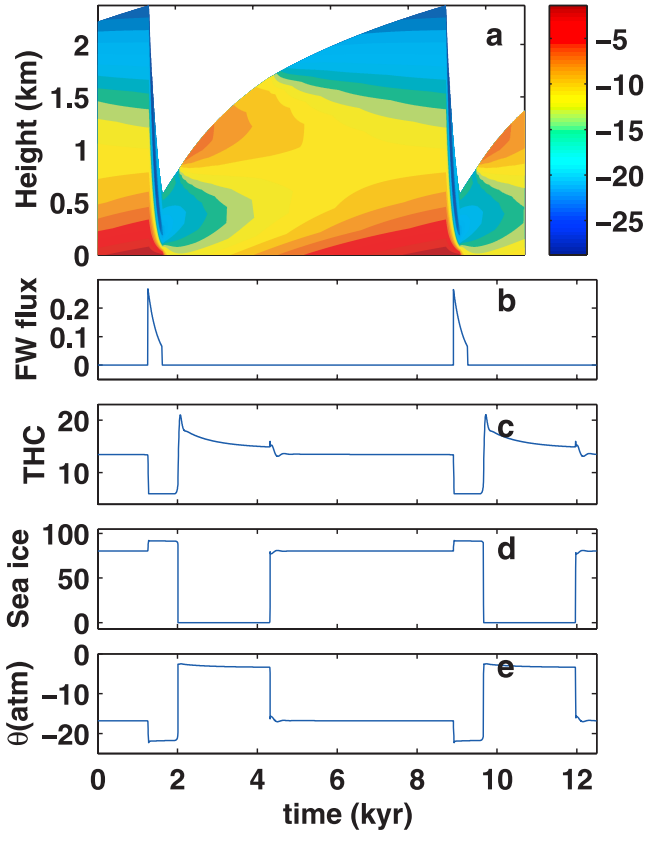

Figure 3. Time series of the different climate subsystems during a full Heinrich event model cycle. (a) Land-ice elevation (km) and the vertical temperature distribution within the ice sheet (degrees Celsius). (b) The freshwater flux released from the ice sheet (Sv). (c) The thermohaline circulation (Sv). (d) Sea-ice extent (percent of northern ocean area). (e) Averaged high-latitude atmospheric temperature (degrees Celsius).

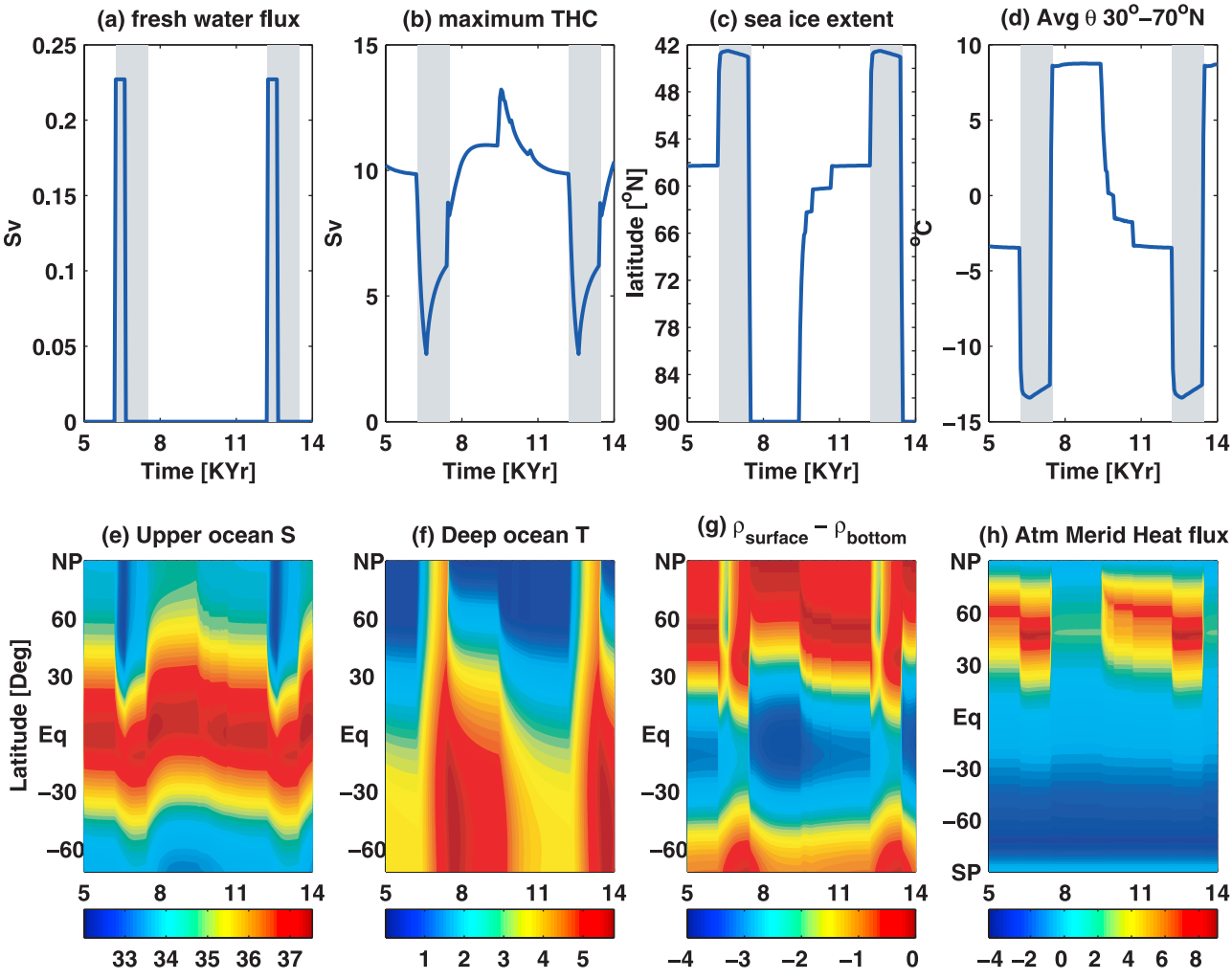

Figure 4. The three sea ice state mechanism for the Heinrich cycle in a coupled model with a continuous meridional resolution. Periodic freshwater (glacier) discharge is specified in this model, and the response of the ocean, sea ice, and atmosphere is calculated and shown here. A detailed model description is provided in Appendix A. This model experiment demonstrates that the triple sea ice state response to glacier discharges, which was seen in the simpler box model of Figure 1 also occurs in this fuller, continuous, model. The upper panels show model time series for (a) the specified freshwater (glacier discharge) input into the northern region of the ocean model, (b) the maximum THC in the Northern Hemisphere, (c) sea ice extent in the Northern Hemisphere (latitude of southernmost point covered with sea ice), (d) averaged atmospheric temperature from 30°N to 70°N showing the atmospheric response to the sea ice switches. The cold periods are highlighted by the gray bands. The lower panels show contour plots of model results as function of both latitude and time: (e) upper ocean salinity (ppt), (f) deep ocean temperature (degree C), (g) density difference between the upper and lower ocean layers (Kg m^{-3}), and (h) the atmospheric meridional heat flux (PW) is shown in panel.

reached the melting point. Consider now the way this ice sheet oscillation combines with the ocean, atmosphere, and sea ice climate components to form our proposed triple sea ice state mechanism for the complete Heinrich cycle.

[13] Initially, the ice sheet is growing, the atmospheric temperature is at cold, glacial values (year 5000 in Figure 3e; year 11,000 in Figure 4d), and the sea ice cover is at its first equilibrium, corresponding to quite an extensive cover (Figures 3d and 4c). Next, once the base reaches the melting temperature, the ice sheet collapses (year 8900, Figure 3a) and releases a meltwater pulse (year 8900 Figure 3b; year 12,000 in Figure 4a) of 0.1–0.25 Sv, matching the observational estimates of *Alley and MacAyeal* [1994]. The freshwater pulse reduces the North Atlantic salinity and causes the THC to weaken somewhat (Figures 3c, 4b, and 4e). The weaker THC results in a reduced heat transport into the northern North Atlantic and therefore allows the sea ice to expand into a yet more extensive area than during normal glacial conditions (Figures 3d and 4c). This is the second out of three sea ice states that compose the entire Heinrich cycle.

The expansion of sea ice and its effects on the increase of surface albedo and reduced air-sea fluxes result in a cooling of both the atmosphere (Figures 3e and 4d) and the ocean. This cooling results in the rapid (a few decades long) sea ice expansion and atmospheric cooling seen in Figures 3d, 3e, 4c, and 4d. This cooling can then propagate to the subtropics, as observed by *Bard et al.* [2000] and *Sachs and Lehman* [1999], via atmospheric meridional heat flux (Figure 4h). This observed cooling supports our sea ice mechanism yet may also be due to other factors such as cold iceberg meltwater carried there by ocean currents. We also note that the amount of subtropical cooling, and its effect on the meridional gradients, seems different for each Heinrich event and that some events are not registered as a major cooling in some sediments cores in relevant regions [*Chapman and Maslin*, 1999].

[14] Such rapid sea ice growth as seen here is expected and occurs during the seasonal cycle in the present-day Southern Ocean, as well as seen in more complex and realistic models. The sea ice expansion is self-limiting as it insulates the ocean from the cold atmosphere and eventually halts the freezing of seawater and creation of additional sea ice [*Gildor and Tziperman*, 2000]. We note that the rapid sea ice switches occur in both the box and continuous models and are also not a result of the model formulation: the timescale for sea ice growth and melt used in the box model is 1 year, and the effect of changing this parameter to 10 years or 1 month is negligible [*Kaspi*, 2002]. The role of such rapid sea ice changes in various rapid climate change events was also raised in some previous works [*Adams et al.*, 1999; *Broecker*, 2000; *Dansgaard et al.*, 1989; *Gildor and Tziperman*, 2000].

[15] The weaker THC allows heat to diffuse from the midlatitude surface ocean into the deep midlatitude ocean, and then into the deep polar ocean, building a reservoir of heat below the surface of the polar ocean (Figure 4f), as has been seen in many three-dimensional (3-D) and other model studies of the response of the THC to freshwater inputs [*Weaver et al.*, 1993; *Winton and Sarachik*, 1993; *Winton*, 1997; *Paul and Schulz*, 2002]. When the collapse of the ice sheet ends (and with it the strong freshwater flux into the ocean; year 9300 in Figure 3b; year 6400 in Figure 4a), the salinity and therefore the density of the surface polar ocean can increase owing to advection and diffusion from the high-salinity midlatitude ocean (Figure 4e). The density of the high-latitude surface water increases after a few hundred years above that of the deeper water, and this leads to convective mixing with the warm subsurface water (Figure 4g), as also seen in general circulation model (GCM) studies [*Weaver et al.*, 1993; *Winton and Sarachik*, 1993]. The deep heat reservoir, brought by the convective mixing to the surface, initiates a melting of the sea ice cover, which is then amplified by the albedo and insulating sea ice feedbacks and results in widespread melt within a few decades. The sea ice melt causes a rapid and strong atmospheric warming to near interglacial values (year 9700 in Figure 3). This brings us to the third oscillation phase, with a very reduced sea ice cover. The salinity, and hence density, increase of the high-latitude surface water at the end of the collapse stage of the ice sheet also creates a modest THC increase (Figure 3c, year 9700; Figure 4b year 7500).

[16] In both of our models the sea ice extent reduces nearly completely during the warm events, but in reality we expect that a moderate reduction in sea ice cover around Greenland would suffice to explain the observed warming. Similarly, the other sea ice states simulated by our models should be taken as qualitative predictions only. It would be preferable if one could initiate our model with a modern LGM reconstruction [*Pflaumann et al.*, 2003], yet our idealized geometry does not permit this. Another critical issue is that of seasonality. Our model neglects seasonal effects, and therefore sea ice extent should be interpreted as winter extent, while sea ice proxies [*Weinelt et al.*, 1996; *DeVernal and Hillaire-Marcel*, 2000; *Sarnthein et al.*, 2000] generally show that seasonality in sea ice during the LGM was quite significant, and so do some model experiments [*Seidov and Maslin*, 1996]. Clearly the highly idealized geometry of our models makes the results only qualitative.

[17] The robust qualitative message of our proposed mechanism, however, is that large-amplitude atmospheric temperature changes are triggered by sea ice changes, via the dominant sea ice albedo and insulating feedbacks, rather than by large-amplitude changes to the THC and its meridional heat transport [*Ganopolski and Rahmstorf*, 2001]. The meridional heat flux by the ocean during the small THC flushes (increases) seen in our somewhat less idealized model, Figure 4, increases from an ambient glacial value of 1.8 to 2.1 Pw at the latitude of maximum THC. This is an increase of some 15% only, and only its amplification by the sea ice melting results in the large atmospheric temperature response. Clearly, these numbers are not to be taken literally, owing to the crudeness of these models, but only as an indication of the weak THC needed to excite the sea ice response. Similarly, dramatic sea ice melt events are initialized by the heat released from the deep ocean by the convective mixing and amplified by the above sea ice feedbacks, rather than caused by large increases in the northward heat transport by the THC. The three sea ice phases of our proposed mechanism also correspond to three THC phases as indicated by proxy observations [*Alley et al.*, 1999] (Figures 3c and 4b), but we emphasize here that sea ice is the main player as far as the atmospheric temperature signal seen in ice cores [*Dansgaard et al.*, 1993] is concerned.

[18] Next, as the insulating sea ice cover is minimized, the surface polar ocean temperature can be efficiently cooled by the atmosphere, and the deep high-latitude oceanic heat reservoir begins to be eliminated by the convective mixing with the cooled surface water. The ocean cooling initially creates a slow atmospheric cooling signal (Figure 3e, years 9700–12,000; seen somewhat better in some of the sensitivity runs of Figure 5) that is also seen in the Greenland ice core records [*Dansgaard et al.*, 1993; *Alley*, 1998]. Eventually, after a few hundred years of slow surface cooling, the deep midlatitude ocean is cooled as well. Once the surface water is sufficiently cold, a rapid sea ice buildup occurs, strongly amplified by the atmospheric cooling due to the sea ice albedo, and the sea ice cover is back to normal glacial values within a few decades. This ends the warm event

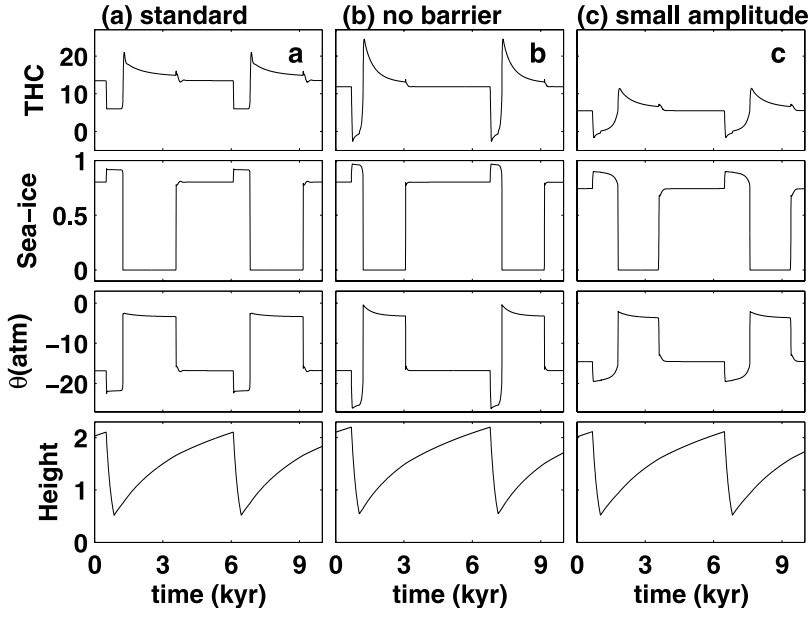

Figure 5. Demonstrating that the triple sea ice state Heinrich cycle mechanism is not sensitive to details of the thermohaline circulation response. (a) The standard model run; (b) a case in which the THC is allowed to vary below 6 Sv (see text). (c) A model run in which, although the amplitude of the thermohaline circulation variability is very small (obtained by tuning of some of the model parameters [*Kaspi*, 2002]), the triple sea ice state cycle still remains unchanged. For each experiment the figure shows time series of the thermohaline circulation (Sv), sea ice extent (percent of northern ocean area), average high-latitude atmospheric temperature (degree Celsius), and glacier height (km).

(year 12,000 in Figure 3d; year 9500 in Figure 4d), and the THC decreases slightly back to normal glacial values. The entire system is back to its initial state, and the cycle repeats. The complete consistency of the simpler box model (Figure 3) and the meridionally continuous model (Figure 4) lend additional reliability to our proposed three sea ice states mechanism.

[19] The mechanism described above is qualitatively similar, in terms of the response of the THC circulation to freshwater forcing, to those proposed by *Winton* [1997], *Paillard and Labeyrie* [1994], and *Ganopolski and Rahmstorf* [2001]. The new element here is that the THC response is very weak and that it is the response of the sea ice which is solely responsible for the observed atmospheric warming above Greenland.

[20] Note that the cold period is triggered here by the glacier discharges. This would imply that initially the glaciers fall into a warm ocean and melt relatively rapidly. Once the THC has weakened, sea ice has expanded, and SST has cooled, the glaciers can survive a longer distance and create the observed IRD tongue in the North Atlantic, which would then be dated to occur within the cold period, as seems to be observed [*Hemming*, 2004].

4. Synchronized Ice Sheet Collapses Around the North Atlantic

[21] We now add a second ice sheet to our coupled box model, representing one of the European ice sheets. This second ice sheet is influenced by the same atmospheric temperature as the first one and, when it discharges, affects the ocean circulation as well. The two glaciers are therefore weakly coupled via their effects on the THC and sea ice and via their mutually felt atmospheric temperature. The second ice sheet is assumed to have a smaller area, and its collapse therefore induces a smaller fresh water pulse into the ocean.

[22] Our mechanism for the synchronized collapses of different ice sheets starts with the observation that a warmer atmospheric temperature at the upper boundary of the ice sheet eventually diffuses toward the bottom of the ice sheet, especially when the ice sheet height is low, as it starts to build up (Figure 3a). This warmer upper temperature makes the ice sheet reach the melting temperature and therefore the collapse stage faster so that it shortens the period of the oscillations [*MacAyeal*, 1993b]. Now a glacier on the east margin of the North Atlantic ocean will generally feel a warmer time-mean temperature than one positioned at the same latitude on the western side (by an average of 2–4°C in our model runs) and should therefore tend to oscillate at a higher frequency (Figure 6a, where the averaged atmospheric temperature felt by the European ice sheet is 2°C warmer). What then makes such two ice sheets discharge glaciers nearly simultaneously [*Elliot et al.*, 1998; *Fronval et al.*, 1995; *McCabe and Clark*, 1998; *Bischof*, 1994; *Jones and Keigwin*, 1988]?

[23] The mechanism we propose here is based on the universal phenomenon of "phase locking" in nonlinear oscillators. The Dutch physicist Huygens noted, as early as the 17th century, that two pendulum clocks weakly coupled by being suspended together from the same

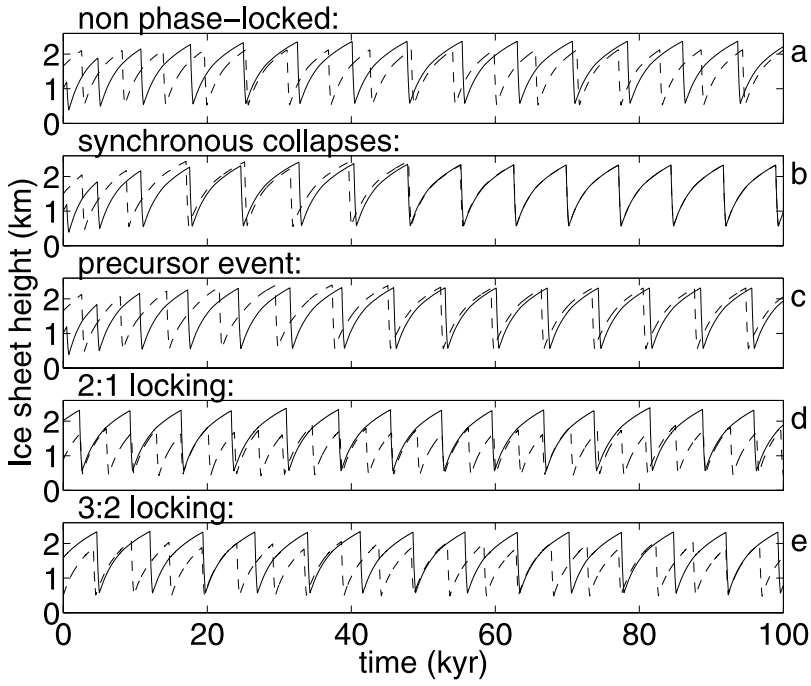

Figure 6. Nonlinear phase locking scenarios as an explanation for the observed synchronous glacier discharges. Shown are time series of the height of two glaciers, a large one (solid lines) representing the LIS and a smaller "European" ice sheet (dash). The two ice sheets are placed in the northern atmospheric model box, and a specified (and different for each run) warm temperature perturbation is added to the atmospheric model temperature felt by the smaller glacier in order to represent the warmer time-mean temperatures in the eastern Atlantic. (a) Two uncoupled glaciers (from two separate model runs) oscillating at different frequencies. (b) Two coupled glaciers starting at different initial conditions, and phase locking at a 1:1 frequency ratio and with no phase lag. The result is synchronous glacier discharge, as seems to be the case for several ice sheets around the North Atlantic [*Bond and Lotti*, 1995; *Elliot et al.*, 1998; *Fronval et al.*, 1995; *McCabe and Clark*, 1998; *Bischof*, 1994; *Jones and Keigwin*, 1988]. (c) Two coupled glaciers phase locked at a 1:1 frequency ratio, such that the smaller one discharges glaciers prior to the larger one, creating a "precursor" event, as seen, e.g., for the Iceland ice sheet [*Bond and Lotti*, 1995]. (d and e) 2:1 (and 3:2) Phase locking in which the smaller glacier oscillates twice for each cycle of the larger one (and three times for every two cycles of the larger one).

supporting frame tend to oscillate synchronously, although when separated, they would slowly drift apart. Two ice sheets located on both sides of the Atlantic, (e.g., the LIS and one of the smaller ice sheets) can be thought of as two clocks with different inherent frequencies due to the different time-mean atmospheric temperature felt by both. The two are weakly coupled together since they both feel similar variations in the atmospheric temperature induced by sea ice expansion and melt events. (In the actual climate system the coupling between ice sheets can also be via the ablation which is also sensitive to the atmospheric temperature variations, or possibly via sea level variations as suggested by *Berger and Jansen* [1994], in the context of the mid-Pleistocene climate shift; see also *Sarnthein et al.* [2000]; *Van-Kreveld et al.* [2000] where this issue is discussed in the context of millennial variability). The glaciers (especially the larger LIS) also affect the atmospheric temperature that is felt by both glaciers via the freshwater pulses they release into the ocean, and that affects the sea ice cover. Figure 6b shows that two such ice sheets, starting from different initial conditions, phase lock fairly rapidly and within a few cycles start oscillating in phase with the same frequency (1:1 phase locking). The time it takes the two glaciers to phase lock could in principle be from one to a few cycle periods and should not be taken as a robust model prediction given the simplicity of our model. The phase locking itself, however, is very robust: we find that a smaller ice sheet, whose period when oscillating by itself may be up to 40% shorter, or up to 10% longer than that of the larger ice sheet, still oscillates synchronously with the larger glacier when coupled. Clearly, more than two ice sheets may be coupled together and phase lock [*Kaspi*, 2002].

[24] Some proxy records indicate that the smaller ice sheets (e.g., the Iceland or European ice sheets) tend to produce small "precursor" events to the larger Heinrich events [*Bond and Lotti*, 1995; *Bond et al.*, 1999; *Grousset et al.*, 2000]. We find that if the difference in the time-mean upper boundary temperature between the glaciers is

increased above some threshold (3–4°C), then the smaller ice sheet still oscillates at the same frequency as the larger one but reaches the collapse stage always before the larger one (Figure 6c), in effect producing a precursor event to the Heinrich event of the larger glacier. This analysis implies that having a precursor event of the Iceland ice sheet does not mean that it necessarily triggers the collapse of the LIS [*Grousset et al.*, 2000]. Rather, the collapses of the Iceland ice sheet, being smaller, may not even have a significant effect on the THC and sea ice cover, so this smaller ice sheet could be only passively phase locked to the atmospheric temperature variations induced by the LIS even though it tends to collapse before the LIS!

[25] This requires a bit of an explanation: Note that the LIS induces no atmospheric temperature change just before it collapses, when the smaller ice sheet collapses. The connection between the two ice sheets does not necessarily occur during the collapse of either of them. The coupling between them is via atmospheric temperature changes induced by the collapses. These temperature changes are felt by the ice sheets, especially right after their collapse, when their thickness is smaller so that atmospheric temperature can penetrate to the bed. Now such a weak connection between the two oscillating glaciers couples them together, causing the synchronous or precursor behavior. We therefore emphasize that the link between the glaciers does not need to be during the collapses themselves but at anytime during the Heinrich cycle. There need not be a direct causal relationship between the LIS and the smaller ice sheet during the collapse of either of them.

[26] Finally, when the smaller ice sheets feel a time-mean upper boundary temperature that is significantly warmer than that of the LIS, their phase locking takes a different form that could also be relevant to the observed IRD characteristics in the North Atlantic. The two glaciers tend to adjust their frequencies in this case so that they relate to each other via the ratio of two integers. For example, if the inherent frequencies are 7200 and 3000 years then, owing to the coupling between them, the two glaciers could oscillate at slightly modified frequencies such as 7000 and 3500 so that the faster one completes exactly two cycles while the slower one completes one (2:1 phase locking, Figure 6d). Additional frequency locking ratios such as 3:2 are also possible, as shown in Figure 6e. The higher frequency D/O oscillations which were originally found in the Greenland ice core [*Dansgaard et al.*, 1993] are now known to also involve ice sheet collapses and IRD discharges from some of the smaller ice sheets around the Atlantic [*Bond and Lotti*, 1995; *Van-Kreveld et al.*, 2000]. Furthermore, the D/O oscillations seem to be part of a larger "Bond cycle" that involves some three D/O events followed by a Heinrich event [*Alley*, 1998]. Could the Bond cycle be a case of some higher phase locking (e.g., 1:4) between the LIS and these smaller ice sheets? Related ideas were also raised by *Schulz et al.* [2002].

5. Sensitivity to the THC

[27] An extensive sensitivity study shows that the above mechanism is very robust to our model parameters [*Kaspi*, 2002]. Consider briefly the sensitivity to the THC that is especially of interest here. Figure 5b shows that the 6 Sv lower limit applied to the THC in our simpler box model (see Appendix A1.2) is not essential for our mechanism, and when applying only the standard linear horizontal density gradient to determine the THC, our mechanism does not change. Furthermore, our triple sea ice state mechanism for the Heinrich cycle is hardly modified even when the amplitude of the THC variations is much smaller than in our standard run (Figure 5c). Note that under warmer, modern climate conditions, sea ice will not expand that far south even when fresh water is injected into the North Atlantic.

[28] The results of the continuous resolution model also support the suggestion that a large-amplitude THC change is not needed in order to explain the atmospheric temperature signal observed as part of the Heinrich and Dansgaard-Oeschger events. Owing to the simplicity of our models, we have emphasized mostly the North Atlantic and ignored the Southern Hemisphere, although there are clearly some obvious teleconnections via the THC that have been explored in many previous studies [e.g., *Seidov et al.*, 2001].

6. Conclusions

[29] The main point of this paper is that sea ice can act as a very efficient amplifier of climate variability. Via its insulating and albedo feedbacks, it can produce significant and most abrupt atmospheric temperature changes, such as observed in the Greenland ice core as part of D/O and Heinrich events. We have shown in particular that a weak thermohaline circulation variability may excite sea ice changes that result in large-amplitude abrupt temperature changes over the North Atlantic.

[30] Our proposed triple sea ice state mechanism accounts for the abrupt warming events [*Bond et al.*, 1993; *Dansgaard et al.*, 1993] following the Heinrich glacier discharge events. As a secondary point, we also showed that synchronous ice sheet collapses are possible due to a weak coupling between the different ice sheets, although as we have explained in the introduction the existence of such synchronous collapses in the proxy record is currently being debated. We saw that while the THC is an important player in the mechanism for the abrupt atmospheric temperature changes, it still acts mostly in a supporting role to that of the sea ice. We could not arrive to these conclusions without using a model that, although simple, includes and couples all relevant components of the climate system. In particular, our mechanism for the phase locking of different ice sheets could not be obtained by specifying freshwater inputs from the ice sheets instead of coupling the ice sheet explicitly to the other climate components. The main aspects of the proposed sea ice amplification of the climate signal caused by the IRD discharges have also been shown here using a model that is continuous in the meridional direction. Furthermore, while both models used here are relatively simple, the different proposed elements of the Heinrich cycle have also been seen in fuller models. For example, a response of the THC to freshwater forcing is seen in coupled ocean-atmosphere GCMs [*Manabe and Stouffer*, 1995], THC

flushes in 3-D models [*Weaver et al.*, 1993; *Winton and Sarachik*, 1993], massive changes in sea ice cover as a result of changes in the ocean heat budget [*Thorndike*, 1992], etc.

[31] Our suggestion that sea ice changes provide sufficient warming at Greenland without a major change to the ocean heat transport are supported by recent atmospheric GCM experiments (C. Li, manuscript in preparation, 2004). We view this as the most robust part of our results. The climate system is also influenced by numerous sources of stochastic noise, which may result in significant freshwater forcing of the North Atlantic [*Hyde and Crowley*, 2002]. Sea ice may be expected to amplify some of this forcing as well to account for more of the observed millennial temperature variability at Greenland.

[32] The implication of all this for future climate change is interesting: If past abrupt and large-amplitude climate changes were indeed due to sea ice feedbacks rather than to THC feedbacks alone, then future climate warming is not likely to cause such large-amplitude abrupt changes, as we clearly do not anticipate an extensive sea ice cover under a global warming scenario.

[33] Besides explaining two major characteristics of the Heinrich cycle, our model also makes some falsifiable predictions that could, in the future, be tested using proxy records. As sea ice proxies [*Weinelt et al.*, 1996; *DeVernal and Hillaire-Marcel*, 2000] improve in accuracy and resolution in the near future, they may be able to verify or falsify our claim that rapid sea ice cover changes triggered the warming and cooling events (as is already hinted in existing proxy records [*Elliot et al.*, 1998]).

Appendix A: Model Description

[34] This paper uses two different models. First, a hemispheric box model that, although simple, couples the dynamics of the ice sheets, atmosphere, ocean, and sea ice (Figure 1; section A1.1), all of which participate in the proposed mechanism. The novelty of this model is in the combination of the different climate subcomponents, while each of these components uses a fairly standard formulation. The model description is therefore appropriately brief, referring to other works for details regarding each of the separate model components. Second, a more detailed pole-to-pole coupled ocean-atmosphere-sea ice-land ice model, which is continuous in the meridional dimension (Figure 2) and is fully described by *Sayag et al.* [2004] with some details specific to the present application, is covered in section A1.2. The land ice is specified and fixed in time in the runs presented in this paper.

A1. Fully Coupled Ice Sheet-Ocean-Atmosphere-Sea Ice Box Model

[35] The coupled box model used here (Figure 1) contains subcomponents for the ocean (thermohaline circulation), atmosphere, sea ice, and land ice. The entire detailed model description is given in the work of *Kaspi* [2002].

A1.1. Land Ice

[36] The land ice model represents the part of the Laurentide Ice Sheet over Hudson Bay and follows *MacAyeal* [1993b, 1993a]. In this model, land ice thickness is assumed to be uniform in the horizontal directions, and the bed on which the land ice lies is assumed to be flat and at sea level. The ice sheet is geothermally heated from below, and once the ice sheet base is melted, the ice is free to slide off the rigid bed into the ocean. The model therefore has two stages: the accumulation (binge) stage while the bed is frozen and the collapse (purge) stage while the base is melted.

[37] The accumulation rate at any given time is determined by the precipitation calculated by the atmospheric model over the northern box and the height of the glacier at that time. We assume that the accumulation rate over the glacier decays exponentially with increasing ice sheet surface elevation to reflect the reduction of precipitable water vapor at higher elevation. The glacier heat equation is a simple diffusion equation in the vertical direction, with the boundary condition being a specified constant geothermal heat flux from below, and a specified upper temperature that is equal to the atmospheric temperature above the ice sheet. The atmospheric model temperature representing a 500 mb level is used to calculate the temperature at the glacier surface using an atmospheric lapse rate of $\Gamma = 9\frac{^{\circ}C}{km}$, as in the work of *MacAyeal* [1993a]. The ablation is considered negligible, as the temperature at the top of the glacier is always less than zero degrees in our runs [*Braithwate*, 1981].

A1.2. Ocean Model

[38] The ocean model is a standard (northern) hemispheric meridional four-box model [*Stommel*, 1961; *Tziperman et al.*, 1994], including a sea ice component as in the work of *Gildor and Tziperman* [2001]. The two upper boxes represent the above thermocline water and are 400 m thick, while the lower boxes represent the deep ocean, with a thickness of 3600 m. Latitude 60°N is the division line between the southern and northern boxes (Figure 1).

[39] The model dynamics include a simple linear frictional horizontal momentum balance and are hydrostatic and mass conserving. The thermohaline circulation is therefore calculated from the meridional density gradient. This parameterization for the THC is rather simple and sometimes results in unrealistic THC reversals. We therefore set a lower limit of 6 Sv regardless of the density gradients. This turns out to be a purely aesthetic fix, as our results are shown in the paper itself to be completely independent of this lower bound, and the more detailed meridionally continuous model does not have this limit and shows no THC reversals.

[40] The equation of state relating the density to the temperature and salinity is the full nonlinear equation recommended by *UNESCO* [1981]. The temperature and salinity for each box are calculated using advection diffusion equations that are forced at the surface by air-sea heat fluxes, and by freshwater fluxes from atmospheric precipitation, glacier runoff (during the purge stage), and sea ice formation and melting. The atmosphere-ocean heat flux term depends on the temperature difference between the atmosphere and ocean and on the depth of the ocean box. In addition, we add a factor that represents the insulating effect of the sea ice. Convective mixing is used to vertically mix the boxes once the vertical stratification becomes unstable.

[41] Sea ice is formed when the ocean temperature drops below a specified freezing temperature and grows also due to atmospheric precipitation falling on the sea ice. The sea ice grows at a constant thickness of 2 m, and its thickness increases only if it covers the entire box area. The sea ice melts when the ocean temperature is above this temperature, as well as due to incoming shortwave radiation [*Gildor and Tziperman*, 2000]. The freezing of ocean water into sea ice and the melting of sea ice are due to a heat flux term proportional to the difference between the ocean temperature and the freezing temperature with a restoring timescale. The model results do not change when this timescale is varied between 1 month and 10 years [*Kaspi*, 2002].

[42] The sea ice plays a major dynamical role via two feedbacks. First, its strong albedo effect dominates the atmospheric energy balance, and second, it insulates the ocean from the atmosphere and significantly reduces the air-sea fluxes where sea-ice cover is present. Thus once sea ice grows, the atmosphere is cooled yet is being insulated from the ocean so that ocean and atmospheric temperatures may significantly diverge.

A1.3. Atmospheric Model

[43] The atmospheric model is a simple two-box energy balance model similar to that of *Nakamura et al.* [1994], *Rivin and Tziperman* [1997] and *Gildor and Tziperman* [2001], in which the horizontal box dimensions coincide with those of the upper ocean boxes. The temperature at a given box is determined by the balance between the incoming shortwave radiation, outgoing longwave radiation, air-sea fluxes, and meridional atmospheric heat fluxes. The albedo used to calculate the portion of the shortwave radiation retained by the atmosphere is due to the separate contributions of the cloud (fixed), sea ice, land, land ice, and ocean albedos.

[44] The meridional freshwater flux is a fairly standard box model formulation, given by *Tziperman and Gildor* [2002, equation (4)], and is different from the atmospheric moisture transport used for studying the glacial-interglacial cycles in the work of *Gildor and Tziperman* [2001]. In the present model the temperature precipitation feedback does not play a critical role as it did in the work of *Gildor and Tziperman* [2001], and the variations in the meridional water flux during the simulated Heinrich event cycle below are very small, in the range of only ±10%.

A1.4. Model Parameters

[45] Following is a list of model parameters whose values are not equal to those in the manuscripts cited for each subcomponent of our coupled model. Starting with the land glacier model, the only addition to that used by *Sayag* [2003], we need to specify the area of the glacier undergoing the binge/purge oscillations (not needed to be specified in *MacAyeal*'s [1993b, 1993a] work), which we set to 10^6 km^2 (note that the area is required in our model, as it controls the amplitude of the freshwater flux due to the binge stage). Taking a glacier area to be anywhere between a third of this size to three times larger, hence modifying the purge freshwater flux into the ocean by a similar factor, does not have any significant effect on the Heinrich cycle mechanism described in the paper.

[46] The ocean model parameters are as in the work of *Tziperman and Gildor* [2002], except that the depth of the upper boxes is set to 400 m; the deep ones to 3600 m; the ocean width to 6300 km; the coefficient relating the THC to the density gradients is 14,300 m^4 s kg^{-1}; the vertical and horizontal diffusion coefficients are 8E-5 m s^{-2} and 8E3 m s^{-2} correspondingly; air-sea flux restoring time is 4 years; and sea ice restoring time is set to 1 year.

[47] The atmospheric model parameters are again as in the work of *Tziperman and Gildor* [2002], except that the Meridional heat coefficient is 1.35E20 J m s^{-1} °K^{-1}; mean daily insolation in the two boxes is (372, 224) Watts m^{-2}; the south and north land albedos are 0.1 and 0.25, respectively, cloud albedo is 0.25; sea ice albedo is 0.55; and ocean albedo is 0.1. The fraction of shortwave used to melt sea ice is 0.25; the emissivities of the south and north boxes are 0.55 and 0.61, respectively; and the meridional freshwater transport coefficient is 7.95E14 m^3 s^{-1}. A sensitivity study for all these parameters is given in the work of *Kaspi* [2002]. The model code is available at http://www.deas.harvard.edu/climate/eli/Downloads/.

A2. Coupled Ocean-Atmosphere-Sea Ice Model With Continuous Meridional Resolution

[48] This model is composed of four coupled submodels for the ocean, atmosphere, sea ice, and land ice. It is continuous in the latitudinal dimension and averaged in the longitudinal dimension and is basically a latitude-continuous version of the box model described above. The model is described in detail by *Sayag et al.* [2004], so we only provide a brief summary of model parameters that are different in the runs presented here. In the atmospheric model component, the land ice albedo is set here to be $\alpha_{LI}^{SW} = 0.6$; the diffusion coefficients in the moisture equation are set to $K_1 = 2.2\ 10^{18}$ m^4/s and $K_2 = 2.2\ 10^{14}$ m^5/s. In the ocean model the thickness of the two layers is $(\Delta_{top}, \Delta_{bot}) = (400,3600)$ m; the horizontal and vertical temperature and salinity diffusion coefficients are $(K_y^T, K_z^T) = (K_y^S, K_z^S) = (4.5\ 10^3, 8\ 10^{-5})$ m^2/s. The portion of longwave radiation that is absorbed by sea ice and results in sea ice melting is $\alpha_{melting} = 0.4$. Finally, the land ice volume does not vary in the runs presented here, and the freshwater pulses are characterized by a flux of 0.75 Sv of fresh water into the ocean for 400 years, followed by a negative (evaporation) flux of 0.075 Sv for 4000 years. The freshwater input into the ocean occurs over a Gaussian profile in latitude, centered at 51°N with a width of 25°; the compensating evaporation flux is centered at the equator with a width of 85°. Other than these, all model parameters are at their original values.

[49] **Acknowledgments.** We thank Mark Maslin, an anonymous reviewer, and Matthew Huber for their most helpful comments on an earlier draft. This work was partially supported by the Israel-U.S. Binational Science Foundation and by the McDonnell Foundation.

References

Adams, J., M. Maslin, and E. Thomas (1999), Sudden climate transitions during the Quaternary, *Progr. Phys. Geogr.*, *23*(1), 1–36.

Alley, R. (1998), Icing the North Atlantic, *Nature*, *392*, 335–336.

Alley, R., and P. U. Clark (1999), The deglaciation of the Northern Hemisphere: A global perspective, *Annu. Rev. Earth Planet. Sci.*, *27*, 149–182.

Alley, R., and D. MacAyeal (1994), Ice-rafted debris associated with binge/purge oscillations of the Laurentide Ice Sheet, *Paleoceanography*, *9*(4), 503–511.

Alley, R., P. U. Clark, L. D. Keigwin, and R. S. Webb (1999), Making sense of millennial-scale climate change, in *Mechanisms of Global Climate Change at Millennial Time Scales*, *Geophys. Monogr. Ser.*, vol. 112, edited by P. U. Clark, R. S. Webb, and L. D. Keigwin, pp. 385–394, AGU, Washington, D. C.

Alley, R., S. Anandakrishnan, and P. Jung (2001), Stochastic resonance in the North Atlantic, *Paleoceanography*, *16*(2), 190–198.

Bard, E., F. Rostek, J. L. Turon, and S. Gendreau (2000), Hydrological impact of Heinrich events in the subtropical northeast Atlantic, *Science*, *289*(5483), 1321–1324.

Berger, W., and E. Jansen (1994), Mid-Pleistocene climate shift: The Nansen connection, in *The Role of the Polar Oceans in Shaping the Global Environment*, *Geophys. Monogr. Ser.*, vol. 85, edited by O. Johannessen, R. Muensch, and J. Overland, pp. 295–311, AGU, Washington, D. C.

Bischof, J. (1994), The decay of the barents ice sheet as documented in the Nordic seas ice-rafted debris, *Mar. Geol.*, *117*, 35–55.

Bond, G., and R. Lotti (1995), Iceberg discharges into the North Atlantic on millennial time scales during the last glaciation, *Science*, *267*, 1005–1009.

Bond, G., et al. (1992), Evidence for massive discharges of icebergs into the North Atlantic Ocean during the last glacial period, *Nature*, *360*(6401), 245–249.

Bond, G., W. Broecker, S. J. Johnsen, J. McManus, L. Labeyrie, J. Jouzel, and G. Bonani (1993), Correlations between climate records from North Atlantic sediments and Greenland ice, *Nature*, *365*, 143–147.

Bond, G., W. Showers, M. Elliot, M. Evans, R. Lotti, I. Hajdas, G. Bonani, and S. Johnson (1999), The North Atlantic's 1–2 kyr climate rhythm: Relation to Heinrich events, Dansgaard/Oeschger cycles and the Little Ice Age, in *Mechanisms of Global Climate Change at Millennial Time Scales*, *Geophys. Monogr. Ser.*, vol. 112, edited by P. U. Clark, R. S. Webb, and L. D. Keigwin, pp. 35–57, AGU, Washington, D. C.

Braithwate, R. J. (1981), On glacier energy balance, ablation, and air temperature, *J. Glaciol.*, *27*(97), 381–931.

Broecker, W. (2000), Abrupt climate change: Casual constraints provided by the paleoclimate record, *Earth Sci. Rev.*, *51*, 137–154.

Broecker, W., and S. Hemming (2001), Climate swings come into focus, *Science*, *294*, 2308–2309.

Broecker, W., G. Bond, M. Klas, E. Clark, and J. McManus (1992), Origin of the northern Atlantic's Heinrich events, *Clim. Dyn.*, *6*, 265–273.

Chapman, M. R., and M. A. Maslin (1999), Low-latitude forcing of meridional temperature and salinity gradients in the subpolar north Atlantic and the growth of glacial ice sheets, *Geology*, *27*(10), 875–878.

Clarke, G. K. C., S. J. Marshall, C. Hillaire-Marcel, G. Bilodeau, and C. Veiga-Pires (1999), A glaciological perspective on Heinrich events, in *Mechanisms of Global Climate Change at Millennial Time Scales*, *Geophys. Monogr. Ser.*, vol. 112, edited by L. D. Keigwin, P. U. Clark, and R. S. Webb, pp. 243–262, AGU, Washington, D. C.

Dansgaard, W., J. White, and S. Johnsen (1989), The abrupt termination of the Younger Dryas climate event, *Nature*, *339*, 532–534.

Dansgaard, W., et al. (1993), Evidence for general instability of past climate from a 250-kyr ice-core record, *Nature*, *364*, 218–220.

DeVernal, A., and C. Hillaire-Marcel (2000), Sea-ice cover, sea-surface salinity and halo-/thermocline structure of the northwest North Atlantic: Modern versus full glacial condition, *Quat. Res.*, *19*, 65–85.

Dowdeswell, J., J. Elverhoi, A. Andrews, and D. Hebbein (1999), Asynchronous deposition of ice-rafted layers in the Nordic seas and North Atlantic Ocean, *Nature*, *400*, 348–351.

Elliot, M., L. Labeyrie, G. Bond, E. Cortijo, J. Turon, N. Tisnerat, and J. Duplessy (1998), Millennial-scale iceberg discharges in the Irminger Basin during the last glacial period: Relationship with the Heinrich events and environmental settings, *Paleoceanography*, *13*, 433–446.

Fronval, T., E. Jansen, J. Bloemendal, and S. Johnsen (1995), Oceanic evidence for coherent fluctuations in Fennoscandian and Laurentide Ice Sheets on millennium timescales, *Nature*, *374*, 443–446.

Ganopolski, A., and S. Rahmstorf (2001), Rapid changes of glacial climate simulated in a coupled climate model, *Nature*, *409*, 153–158.

Gildor, H., and E. Tziperman (2000), Sea ice as the glacial cycles climate switch: Role of seasonal and orbital forcing, *Paleoceanography*, *15*, 605–615.

Gildor, H., and E. Tziperman (2001), A sea-ice climate-switch mechanism for the 100 kyr glacial cycles, *J. Geophys. Res.*, *106*(C5), 9117–9133.

Grousset, F. E., C. Pujol, L. Labeyrie, G. Auffret, and A. Boelaert (2000), Were the North Atlantic Heinrich events triggered by the behavior of the European ice sheets?, *Geology*, *28*(2), 123–126.

Heinrich, H. (1988), Origin and consequences of cyclic ice rafting in the northeast Atlantic Ocean during the past 13,0000 years, *Quat. Res.*, *29*, 142–152.

Hemming, S. R. (2004), Heinrich events: Massive late Pleistocene detritus layers of the North Atlantic and their global climate imprint, *Rev. Geophys.*, *42*, RG1005, doi:10.1029/2003RG000128.

Huang, R. H., J. R. Luyten, and H. M. Stommel (1992), Multiple equilibrium states in combined thermal and saline circulation, *J. Phys. Oceanogr.*, *22*(3), 231–246.

Hyde, W. T., and T. J. Crowley (2002), Stochastic forcing of Pleistocene ice sheets: Implications for the origin of millennial-scale climate oscillations, *Paleoceanography*, *17*(4), 1067, doi:10.1029/2001PA000669.

Jones, G., and L. Keigwin (1988), Evidence from Fram Strait (78 n) for early deglaciation, *Nature*, *336*, 56–59.

Kaspi, Y. (2002), A mechanism for the abrupt warming and simultaneous ice sheet discharge involved in Heinrich events, M.S. thesis, Weizmann Inst., Rehovot.

MacAyeal, D. (1993a), Binge/purge oscillations of the Laurentide Ice Sheet as a cause of North Atlantic Heinrich events, *Paleoceanography*, *8*(6), 775–784.

MacAyeal, D. (1993b), A low-order model of the Heinrich event cycle, *Paleoceanography*, *8*(6), 767–773.

Manabe, S., and R. J. Stouffer (1995), Simulation of abrupt climate change induced by freshwater input to the North Atlantic Ocean, *Nature*, *378*, 165–167.

Marshall, S. J., and G. K. C. Clarke (1997), A continuum mixture model of ice stream thermomechanics in the Laurentide Ice Sheet: 2. Application to the Hudson Strait ice stream, *J. Geophys. Res.*, *102*(B9), 20,615–20,637.

Maslin, M. A., D. Seidov, and J. Lowe (2001), Synthesis of the nature and causes of sudden climate transitions during the Quaternary, in *The Oceans and Rapid Climate Change: dPast, Present, and Future*, *Geophys. Monogr. Ser.*, vol. 126, edited by D. Seidov, B. J. Haupt, and M. Maslin, pp. 9–52, AGU, Washington, D. C.

McCabe, A., and P. Clark (1998), Ice-sheet variability around the North Atlantic Ocean during the last deglaciation, *Nature*, *392*, 373–377.

Nakamura, M., P. H. Stone, and J. Marotzke (1994), Destabilization of the thermohaline circulation by atmospheric eddy transport, *J. Clim.*, *7*, 1870–1882.

Paillard, D., and L. Labeyrie (1994), Role of the thermohaline circulation in the abrupt warming after Heinrich events, *Nature*, *372*, 162–164.

Paul, A., and M. Schulz (2002), Holocene climate variability on centennial-to-millennial time scales: 2. Internal feedbacks and external forcings as possible causes, in *Climate Development and History of the North Atlantic Realm*, edited by G. Wefer et al., pp. 55–73, Springer-Verlag, New York.

Pflaumann, U., et al. (2003), Glacial North Atlantic: Sea-surface conditions reconstructed by GLAMAP 2000, *Paleoceanography*, *18*(3), 1065, doi:10.1029/2002PA000774.

Rivin, I., and E. Tziperman (1997), Linear versus self-sustained interdecadal thermohaline variability in a coupled box model, *J. Phys. Oceanogr.*, *27*(7), 1216–1232.

Sachs, J. P., and S. J. Lehman (1999), Subtropical North Atlantic temperatures 60,000 to 30,000 years ago, *Science*, *286*(5440), 756–759.

Sarnthein, M., et al. (2000), Fundamental modes and abrupt changes in North Atlantic circulation and climate over the last 60 ky concepts, reconstruction and numerical modeling, in *The Northern North Atlantic: A Changing Environment*, edited by S. P. W. Ritzrau, M. Schlutter, and J. Thiede, Springer-Verlag, New York.

Sayag, R. (2003), Rapid switch-like sea ice growth and land ice—Sea ice hysteresis in a continuous coupled model, M.S. thesis, Weizmann Inst., Rehovot.

Sayag, R., E. Tziperman, and M. Ghil (2004), Rapid switch-like sea ice growth and land ice-sea ice hysteresis, *Paleoceanography*, *19*, PA1021, doi:10.1029/2003PA000946.

Schulz, M., A. Paul, and A. Timmermann (2002), Relaxation oscillators in concert: A framework for climate change at millennial timescales during the late Pleistocene, *Geophys. Res. Lett.*, *29*(24), 2193, doi:10.1029/2002GL016144.

Scourse, J. D., I. R. Hall, I. N. Mccave, J. R. Young, and C. Sugdon (2000), The origin of Heinrich layers: Evidence from h2 for European precursor events, *Earth Planet. Sci. Lett.*, *182*(2), 187–195.

Seidov, D., and M. Maslin (1996), Seasonally ice free glacial nordic seas without deep water ventilation, *Terra Nova*, *8*(3), 245–254.

Seidov, D., E. Barron, B. J. Haupt, and M. Maslin (2001), Ocean bi-polar seesaw and climate: Southern versus northern meltwater impacts, in *The Oceans and Rapid Climate Change: Past, Present, and Future*, *Geophys. Monogr. Ser.*, vol. 126, edited by D. Seidov, B. J. Haupt, and M. Maslin, pp. 147–167, AGU, Washington, D. C.

Stommel, H. (1961), Thermohaline convection with two stable regimes of flow, *Tellus*, *13*, 224–230.

Thorndike, A. (1992), A toy model linking atmospheric thermal radiation and sea ice growth, *J. Geophys. Res.*, *97*, 9401–9410.

Timmermann, A., H. Gildor, M. Schulz, and E. Tziperman (2003), Coherent resonant millennial-scale climate oscillations triggered by massive meltwater pulses, *J. Clim.*, *16*(15), 2569–2585.

Tziperman, E., and H. Gildor (2002), The stabilization of the thermohaline circulation by the temperature-precipitation feedback, *J. Phys. Oceanogr.*, *32*, 2707–2714.

Tziperman, E., J. R. Toggweiler, Y. Feliks, and K. Bryan (1994), Instability of the thermohaline circulation with respect to mixed boundary-conditions: Is it really a problem for realistic models?, *J. Phys. Oceanogr.*, *24*(2), 217–232.

UNESCO (1981), 10th report of the joint panel on oceanographic tables and standards, *Tech. Rep. 36*, Paris.

Van-Kreveld, S., M. Sarnthein, H. Erlenkeuser, P. Grootes, S. Jung, M. J. Nadeau, U. Pflaumann, and A. Voelker (2000), Potential links between surging ice sheets, circulation changes, and the Dansgaard-Oeschger cycles in the Irminger Sea, 60–18 kyr, *Paleoceanography*, *15*(4), 425–442.

Wang, Z., and L. Mysak (2001), Ice sheet-thermohaline circulation interactions in a climate model of intermediate complexity, *J. Oceanogr.*, *57*, 481–494.

Weaver, A. J., J. Marotzke, P. F. Cummins, and E. S. Sarachik (1993), Stability and variability of the thermohaline circulation, *J. Phys. Oceanogr.*, *23*, 39–60.

Weaver, A. J., et al. (2001), The uvic Earth system climate model: Model description, climatology and application to past, present and future climates, *Atmos. Ocean*, *39*, 361–428.

Weinelt, M., M. Sarnthein, U. Pflaumann, H. Schultz, S. Jung, and H. Erlenkeuser (1996), Ice-free Nordic seas during the Last Glacial Maximum? Potential sites of deepwater formation, *Paleoclimates*, *1*, 282–309.

Winton, M. (1997), The effect of cold climate upon North Atlantic deep water formation in a simple ocean-atmosphere model, *J. Clim.*, *10*(1), 37–51.

Winton, M., and E. S. Sarachik (1993), Thermohaline oscillation induced by strong steady salinity forcing of ocean general circulation models, *J. Phys. Oceanogr.*, *23*, 1389–1410.

Y. Kaspi, MIT-WHOI Joint Program in Physical Oceanography, MIT, 77 Massachusetts Ave., Cambridge, MA 02138, USA.

R. Sayag and E. Tziperman, Earth and Planetary Sciences, Harvard University, 20 Oxford St., Cambridge, MA 02138-2902, USA. (eli@eps.harvard.edu)